

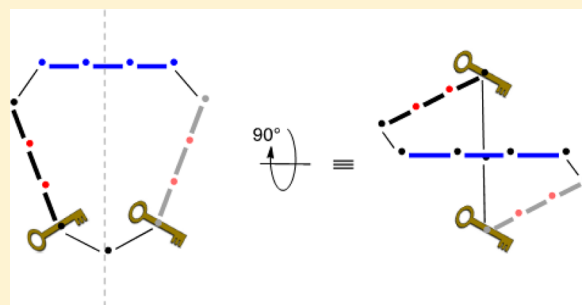
Positioning and Configuration of Key Atoms Influence the Topology of [13]-Macrolides

Jun Ma and Mark W. Pecuh*

Department of Chemistry, University of Connecticut, 55 North Eagleville Road U3060, Storrs, Connecticut 06269, United States

Supporting Information

ABSTRACT: Key atoms at specific positions along the ring govern the shape, or “topology” of a group of [13]-macrolides. Here we report the synthesis of these macrocycles and their characterization by functional and structural methods. The [13]-macrolides are organized by three four-atom planar units that help to rigidify them and one hinge atom that enables the planar units to orient themselves. The driving force for the organization of the structures is the minimization of steric strain on groups attached to the key atoms. When the key atom is a stereocenter, a macrocycle with planar chirality is observed. An alternative cup-like topology arises when the key atom bears two alkyl groups. Additionally, the key atoms can work in a coordinated fashion to guide one topology over another. The synthesis relied on an acylation-ring closing metathesis sequence. Rigidity was demonstrated by variable-temperature NMR experiments and diastereoselective epoxidation reactions. X-ray crystal structures of representative [13]-macrolides served as the basis of the structural observations made. The results provide a framework for the design of new macrocycles with well-defined structures as well as for understanding some general principles that influence the topology of natural product macrocycles.



INTRODUCTION

Macrocycles are a versatile class of compounds with applications in medicinal chemistry, chemical biology, and materials science. Nature has identified many macrocyclic compounds with potent biological activity, for example. A short list of natural product macrocycles with diverse activities includes erythromycin (antibacterial), amphotericin (antifungal), rapamycin (immunomodulatory), epothilone (anticancer), and bryostatin (memory/anti-Alzheimers).¹ These compounds are either used in the clinic presently or are undergoing clinical trials for the activities listed. Their effectiveness as therapeutics has certainly motivated the development of analogs. In fact, over 100 marketed macrocyclic drugs are, or are derived from, natural products.² Azithromycin is an excellent example of how derivatization of a natural product, in this case erythromycin, expanded the scope of its therapeutic potential.³ Peptide sequences where natural or un-natural amino acid side chains are covalently linked to form a macrocycle also fit into this category. The formation of a macrocycle in these instances helps to restrict the conformational space adopted by the peptide and enables the sequence to bind a target protein and inhibit important protein–protein interactions.⁴

Due to their novel mechanisms of action and their success as therapeutics, natural product and natural product analog macrocycles have kindled broad interest in the synthesis⁵ and characterization of natural-product-like macrocycles.⁶ This class of compounds is different because it is not directly related to a specific natural product but is merely motivated by similar (perceived) design principles. Common ring sizes observed for

these macrocycles are 12–14 atoms. They are attractive for investigation as potential drug candidates because they occupy a molecular space somewhere between traditional small molecules and biologics. Their size allows them to bind to extended sections of a target protein with the promise of higher selectivity and potency. They have reduced flexibility relative to acyclic molecules of similar molecular weight; the rigidification contributes to the selectivity in binding of macrocycles.

A related question is how certain factors such as planar units (e.g., esters, amides, etc.) and the location of stereocenters along the ring govern the overall shape of a macrocycle.⁷ The absolute configuration of atoms at specific places along the ring (key atoms) determines how a molecule folds in its acyclic form en route to the macrocycle. Such centers have been termed sigma elements.^{8,9} They are critical to linking local stereochemistry to the overall topology of a macrocycle. The function of a macrocycle is intimately associated with its structure, so having a clear understanding of how shape propagates in macrocycles will aid in the design of ligands for specific protein targets, provide guidance in the design of diversity oriented synthesis campaigns, and also provide a context for predicting the shapes of natural product macrocycles in the absence of crystallographic or extensive spectroscopic data.¹⁰

We recently reported on a group of [13]-macrolactones that possess a planar chirality by virtue of the interplay among three planar units, a hinge atom, and the absolute stereo-

Received: February 26, 2013

Published: June 26, 2013

chemistry of a single asymmetric carbon.^{11,12} In the initial investigation, where the macrolactone ring was fused to a pyranose ring through C4 and C6 hydroxyl groups, we demonstrated highly stereofacial epoxidation reactions. Switching the absolute configuration at C4 (D-glucose to D-galactose) resulted in the presentation of the opposite diastereoface of an embedded alkene unit. Separate X-ray crystal structures of the D-galactose fused macrocycle as both the alkene **1** and epoxide **2** (Figure 1) showed that the selectivity arose from the fact that

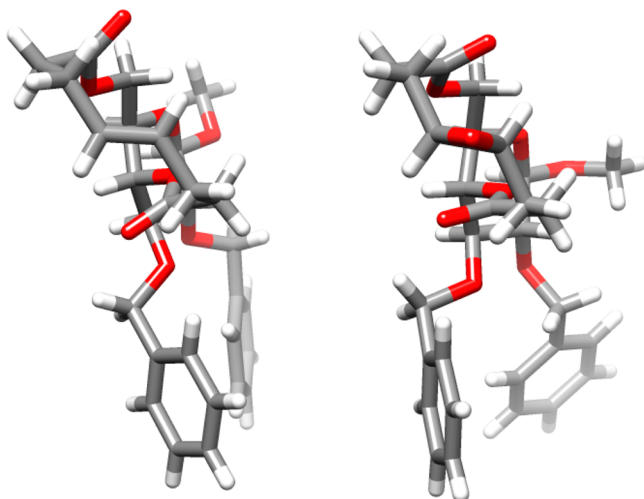
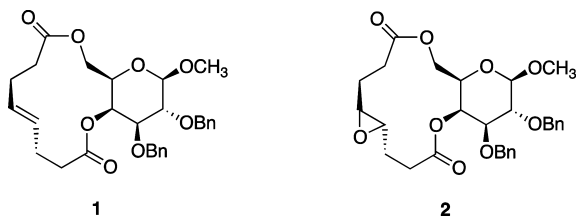


Figure 1. X-ray crystal structures of **1** and **2** depicting the planar chirality of the [13]-macrodilactones.

the [13]-macrolactone backbone was twisted and the π -bond of the alkene was perpendicular to the twist axis. This meant that there was an inside and an outside face of the alkene. Only the outside diastereoface¹³ reacted with the epoxidation reagent, DMDO. Subsequent work¹² pared down the features of the pyranose that were responsible for the planar chirality.¹⁴ Synthesis of minimalist, chiral hydroxymethyl cyclohexanol “pseudo-enantiomers” of the D-glucose and D-galactose fused [13]-macrolactones led to the conclusion that just one key stereocenter contributed to the planar chirality of the [13]-macrolactones. An X-ray structure of the racemic [13]-macrolactone **3** confirmed that one asymmetric carbon governed the planar chirality—the topology—of the macrocycle.



[13]-Macrolactone **3a** (Figures 2 and 3) contains two ester units, C12–C13–O1–C2 (dihedral angle = 178.5°) and C4–O5–C6–C7 (175.1°) and one alkene (C8–C11, 174.8°). A scheme that defines atom numbering for the [13]-macrodilactones is provided in Figure 4. The esters of **3a** are in a typical *s-trans* conformation and the *E*-alkene is in a relatively similar orientation. These three planar units, each containing four atoms, account for 12 of the 13 atoms of the macrocycle. As has been pointed out for 12-membered macrocycles, planar units are effective means for rigidifying the ring.⁷ The remaining

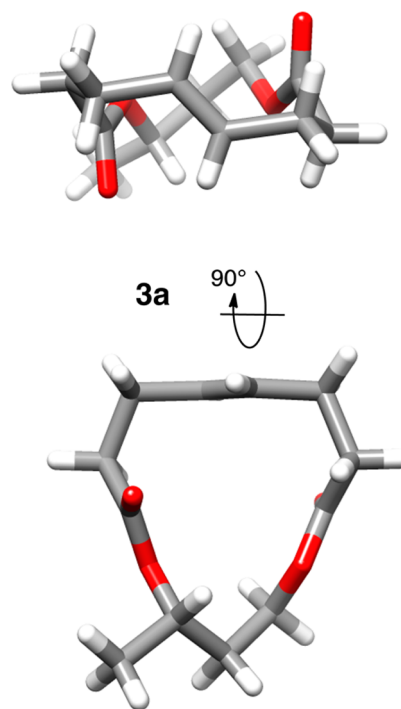


Figure 2. Crystal structure of the *S*-enantiomer [13]-macrodilactone **3a**. The *R*-enantiomer (not shown) is also present in the unit cell of the crystal.

atom in **3a**, C3, is not part of any planar array. Rather, the planar units organize around this center to minimize steric interactions between the group attached to the chiral center, C2, and the rest of the ring. We referred to this carbon (C3) as the hinge atom to emphasize how the planar units flex around it with a specific screw-sense. A substituent as small as a methyl group on C2 was sufficient to direct the fold of the [13]-macrolactones.¹¹ Here we follow up on that observation and evaluate how both the planar units and key atoms in the backbone affect the fold of the novel [13]-macrodilactones through a two-pronged approach. First, we evaluated the dynamics of the [13]-macrodilactones by inspecting select ¹H NMR spectra and evaluating the selectivity of epoxidation of the alkene unit embedded in their structure. Second, we inspected the structures of several [13]-macrodilactones that were collected by X-ray crystallography. The data show that the interplay of these features works together to govern macrocycle topology and has implications for drug design and natural product chemistry.

RESULTS AND DISCUSSION

The [13]-macrodilactones **3a–i** were synthesized by an acylation–ring closing metathesis (RCM) route (Scheme 1). Diversity among the product [13]-macrodilactones originated from the bis-functionalized starting materials **4a–i** used. They consisted of simple diols (**4a**, **4b**, **4d**, and **4h/4i**),¹⁵ amino alcohols (**4e**, **4f**), and diamines (**4c**, **4g**). Each starting material was commercially available, although we chose to synthesize **4g** from 3-aminobutanoic acid via a modified procedure (see Experimental Section for details on the synthesis of **4g**).¹⁶ Both ends of the diols, amino alcohols, and diamines were acylated with 4-pentenoic acid using DCC as a coupling reagent and DMAP as catalyst. Yields for the bis-acylation ranged from 46 to 99%. Using conditions previously established for the RCM of

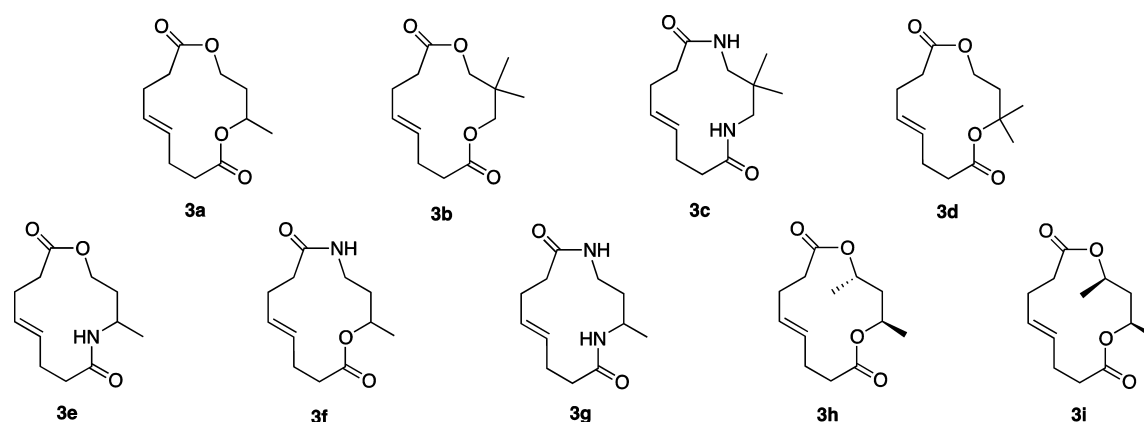


Figure 3. [13]-Macrolidides 3a–i. Table 1 reports the yields for synthesis and reaction of each compound.

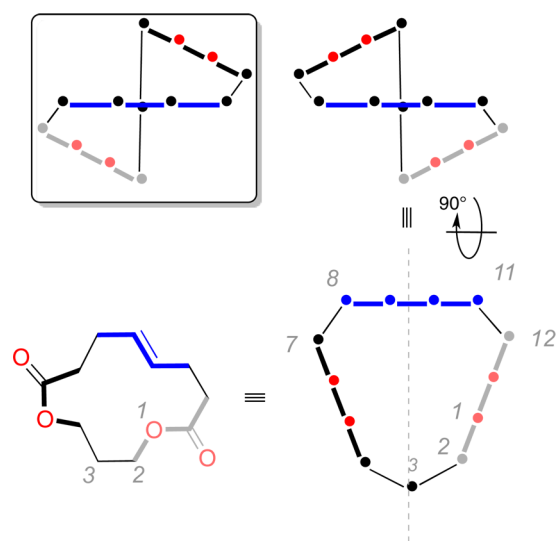
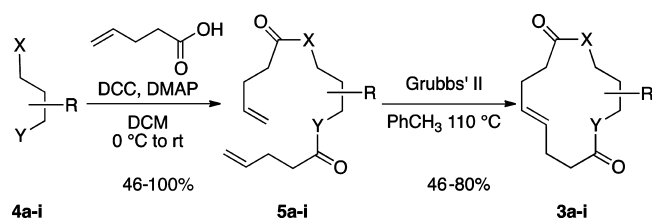


Figure 4. General representation of the [13]-macrolidide structure (with numbering used in the manuscript) that emphasizes the planar motifs and their organization.

Scheme 1



[13]-macrolidides,¹² the dienes 5a–i were converted to macrocycles 3a–i (61–80%) as illustrated in Figure 2. Macrocycles 3a–i were also hydrogenated to provide completely saturated [13]-macrolidides 6a–i (Scheme 2). Yields for the acylation, RCM, and hydrogenation reaction for each series are collected in Table 1. The hydrogenation reaction aided in confirming the structure of the parent compounds and also demonstrated that the embedded alkenes could be reactive under standard conditions. Hydrogenation of the alkene destroyed one of the planar units in the macrocycle. We suspected that the saturation of the alkene unit may have observable physical ramifications for the ring dynamics.

To gather information about the ring dynamics of the alkene-containing [13]-macrolidides (3) and the reduced analogs 6, we

Scheme 2

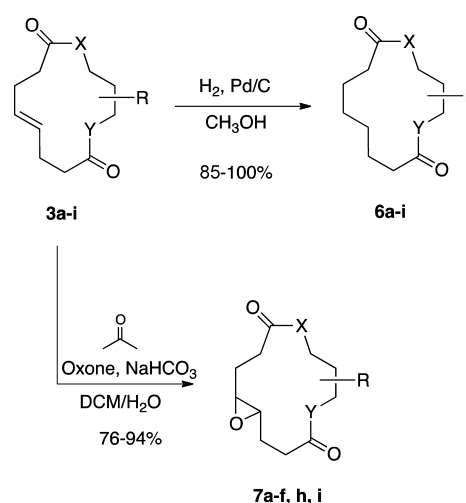


Table 1. Yields of Cyclization and Subsequent Reactions of Embedded Alkene by Macrocycle

series	acylation (%) 5	RCM (%) 3	hydrogenation (%) 6	epoxidation (%) 7
a	87 ^a	72 ^a	85	93
b	90	61	92	88
c	99	46	99	81
d	100	67	99	77
e	65	80	100	93
f	97	61	98	76
g	46	72	98	- ^c
h	72 ^b	50	88	94
i		26	99	91

^aYields for 5a and 3a are from ref 23. ^bSynthesized as a mixture of the racemic and meso diastereomers. ^cEpoxidation of 3g under the standard conditions was not successful.

collected variable temperature (VT) ¹H NMR data¹⁷ on compounds 3h and 6h.¹⁸ The spectra of 3h were very similar at rt and 50 °C. There were minor chemical shift changes and the signals that correspond to the C2, C4, and methyl hydrogens showed some broadening at 50 °C. Signals for the other protons were essentially unchanged which suggested a relatively rigid structure. For 6h, there were slight chemical shift changes and also some minor changes in coupling constants. A significant indicator, however, was the observation that signals

corresponding to the alkane region (e.g., C9, C10) apparently coalesced between 50 and 75 °C. The interpretation of the data for **6h** was that the structure was relatively rigid at room temperature but that multiple conformations were accessed, particularly in the C8–C11 region at the higher temperatures. Overall, the VT experiments lent support to the notion that the parent [13]-macrolide structures were rigid due primarily to the planar units present in their backbone.

High facial selectivity in reactions involving the embedded alkene unit was observed among the [13]-macrolactones that we previously studied.^{11,12} Specifically, epoxidations of **1** and related (chiral) compounds were shown to be highly diastereoselective. The observed selectivity acted as a functional read-out for the ring dynamics of the macrocycles. Low selectivity in reactions of the double bond would indicate free rotation around the alkene unit because the rotation would expose both faces to reaction. Conversely, high facial selectivity would suggest a more rigid structure. We therefore opted to perform epoxidation reactions on **3a–i** as an additional method for assessing their rigidity.

It is important to clarify the relationship between point chirality and planar chirality of **3a–i** before undertaking the analysis of the products of epoxidation. The interrelationship between these chiralities defines the topology of the [13]-macrolides being studied. We are using planar chirality here, as others have,¹⁹ to connote the nonplanarity or twist of the macrocycle. The point chirality of a key stereocenter will govern this planar chirality. The starting materials for the synthesis of the [13]-macrolides fall into two groups: (i) 1,3-butanediol **4a**, 3-amino-1-butanol **4e**, 4-amino-2-butanol **4f**, 1,3-diaminobutane **4g**, and 2,4-pentane diol **4h**^{20,21} were used as their respective racemic mixtures; (ii) 2,2-dimethyl-1,3-propanediol **4b**, 2,2-dimethyl-1,3-diaminopropane **4c**, 1,1-dimethyl-1,3-propanediol **4d**, and *meso*-2,4-pentanediol **4i** are achiral. We expected that macrocycles synthesized from achiral starting materials would either adopt a racemic mixture of enantiomeric planar chiralities or they would potentially adopt some new topology that was symmetric and therefore achiral too. Macrocycles prepared from racemic starting materials (point chirality) were simply expected to be racemic via the propagation of enantiomeric planar chiralities. In this case, each enantiomer of the starting material would directly correspond to one specific planar chirality. The twist of each enantiomeric macrocycle in the racemate would be determined by the absolute configuration of the key atom. Despite the fact we were studying these compounds in the optically inactive series, we expected to learn about the structures and their dynamics. The lessons are directly applicable to either asymmetric series; that is, if the synthesis began with an optically active starting material, then the topology of the macrocycle could be predicted based on the starting material's absolute configuration. Regardless of the exact topology adopted by [13]-macrolides **3a–i**, the products of their epoxidation were, by definition, not expected to be optically active either. Diastereomeric epoxides would arise only if the planar alkene unit was rotating or oscillating to expose both reactive faces, which was not expected.

The procedure for epoxidations in this study used *in situ* generated DMDO as the epoxidizing reagent (Scheme 2).⁷ While we used the same reagent in our previous studies,^{11,12} it was prepared separately and added into the epoxidation reaction. We chose the *in situ* method for its convenience and because others had shown that this method could

selectively and efficiently epoxidize alkenes embedded in macrocycles. In all cases but one, a single diastereomeric series of epoxides **7a–i** was obtained. Repeated attempts to epoxidize **3g** under the standard conditions, as well as others,²² were unsuccessful. Data from chromatography and ¹H and ¹³C NMR experiments supported the conclusion that a single diastereomer was produced in each epoxidation. These epoxidation results were consistent with a model where the embedded alkenes reacted via their outside face only and, further, that [13]-macrolides were in fact rigid.

Through inspection of the structure obtained from X-ray crystallographic data for [13]-macrolactone **3a** (Figure 2), several key characteristics important to the topology of this ring system became apparent. Because racemic 1,3-butanediol was used in the synthesis, both enantiomers were present in the unit cell; here only one of the enantiomers is analyzed, but the principles are applicable to both. Further, the new compounds we report here, especially the structures derived from X-ray data on **7b** and **7d**, and **3h** and **3i**, helped to illustrate and refine our understanding of the characteristics. As outlined above, the planar chirality of **3a** can be attributed to its three planar units, the hinge atom, and the absolute stereochemistry of the chiral center. The stereochemistry at C2 in **3a** is the crucial determinant for the planar chirality of the folded macrocycle. This is because C2 is in an eclipsing conformation with the carbonyl oxygen of its planar ester unit. Depending on the configuration of that center, the substituents attached to it will either be pointing into the macrocycle or away from it when it adopts the twisted conformation. The substituent is too big to occupy a site inside the macrocycle and so the ring (presumably pre-established in its acyclic form) wraps around to accommodate it on the outside of the developing ring.

C2 is not the only atom that is able to dictate the folding of the [13]-macrolide structures; there are other key stereocenters along the chain of the macrocycle (Figure 4). C4 is an ester carbon analogous to C2, for example, and the chirality of this center could work synergistically with C2 or it could interfere with it. The α -carbons of both esters (C7 and C12) and the carbons that are adjacent to the alkene at C8 and C10 are also at positions of the molecule's backbone that are akin to C2 and C4. That is, they are at the junction of two planar units and may therefore exert an influence on macrocycle topology in the same way as C2. Each of these centers could either work constructively to reinforce a given fold or they could work against each other. This could potentially result in alternative ring topologies. Based on an axis of symmetry, on the other hand, C3 should have no effect on the fold of the macrocycle. Comparison of the X-ray crystal structures of **7b** and **7d** helps to illustrate some of these features.

The structure on the left in Figure 5 corresponds to compound **7b**, the epoxidation product of macrocycle **3b**. The fact that it is the macrocyclic epoxide rather than the corresponding alkene requires some qualification because X-ray structures containing either of these functional groups will be compared to each other interchangeably. First, the structure illustrates the inside–outside disposition of faces on the erstwhile alkene. Reaction occurs only on the outside face of the alkene because the interior space of the macrocycle is too small to host a reagent molecule.¹³ Second, the ring topology between alkene and epoxide is conserved for [13]-macrolides. This argument is based on earlier X-ray data collected in our group for the D-galactose-fused macrocycle as the alkene and epoxide (Figure 1). The only difference between structures

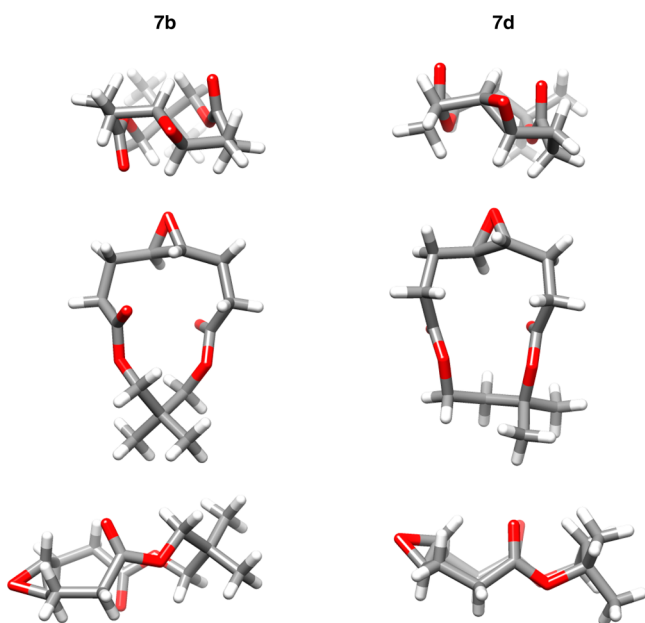


Figure 5. X-ray crystal structures of [13]-macrodialdehydes **7b** and **7d**.

1 and **2**, aside from the epoxide oxygen atom itself, is the compactness of the macrocycle. The distance between the ester carbonyl oxygens illustrates this. For **1**, the distance is 5.153 Å and for **2** it is 4.289 Å. The correspondence between the shape of structures **1** and **2** means that analysis of the X-ray structure of the epoxide **7b** is essentially the same as for alkene **3b** and we can infer structural information about the alkene through inspection of the epoxide. Substitution on the macrocyclic ring of **7b** is at the C3 position, a position that, in our analysis above, should have little or no consequence on the specific fold adopted by the macrocyclic ring. Inspection of **7b** shows that it adopts the typical ribbon shape that is reminiscent of the original [13]-macrodialdehydes. In fact, structures of both enantiomeric planar chiralities are present in the unit cell. This indicates that the ribbon fold is likely the lowest energy configuration for the [13]-macrodialdehydes and also that the C3 position has no influence on which planar chirality is adopted within that fold.

Also shown in Figure 5 (on the right) is the X-ray crystal structure of macrocyclic epoxide **7d**. It too contains a geminal dimethyl unit along the macrocyclic backbone but in this case it is at the C2 position. We suspected that if a ribbon topology were to be adopted for **7d**, then one of the two methyl groups would be forced to be inside the macrocyclic ring. Instead, **7d** adopts an alternate topology all together. The topology is more cup-shaped rather than a ribbon fold, although the planar chirality is still present. The difference in overall topology is best illustrated in lower side-view images of **7b** and **7d** in Figure 5. From this perspective, the cup shape is plainly evident. The planar units are maintained, but their arrangement is changed by a reorganization of the diol unit. For example, the ester carbonyls in the cup configuration (**7d**) are parallel to each other whereas they are antiparallel in the ribbon (**7b**). Significantly, the three carbon atoms that are part of the backbone of the macrocycle become nearly coplanar themselves in **7d**, which creates an adventitious fourth planar unit. The O1–C2–C3–C4 and C2–C3–C4–O5 dihedral angles for this part of the molecule are -62.12° and 66.63° , respectively. For **7a**, the same angles are 50.61° and 50.61° ; these angles give rise

to the screw-sense of the planar chirality in the ribbon configuration. Nonetheless, **7d** still contains an attenuated planar chirality. That is, the orientation of the alkene unit from C8–C11 adopts two configurations, each of which creates a planar chirality.²⁴ The unit cell once again has copies of both enantiomers. It is the absence or presence of the screw-sense in the diol unit, then, that guides the overall topology of the macrocycle.

It also became apparent that the key atoms can also work together constructively to reinforce a given topology based on their absolute configuration. Compounds **3h** and **3i** were prepared to test this possibility. A commercially available mixture of racemic and *meso*-2,4-dimethyl-pentane-1,3-diol was acylated under the standard conditions to provide racemic **5h** and *meso* diester **5i**. The components of this mixture could not be separated. Rather, the mixture carried through the RCM reaction, then **3h** and **3i** were separated by column chromatography. Based on the previous X-ray structures, we reasoned that [13]-macrodialdehyde **3h** would adopt the ribbon configuration (e.g., **3a**, **7b**) because the methyl groups at the C2 and C4 stereocenters, respectively, could sit on the outside the macrocycle. This was because the absolute configurations of these centers were complementary to the topology. By the same logic, *meso* compound **3i** would be akin to **3d** or **7d**. Methyl groups at C2 and C4 on this compound would be best accommodated by the more elongated or flattened planar chirality as observed for **7d**. Structures derived from X-ray crystallographic data for **3h** and **3i** are shown in Figure 6.

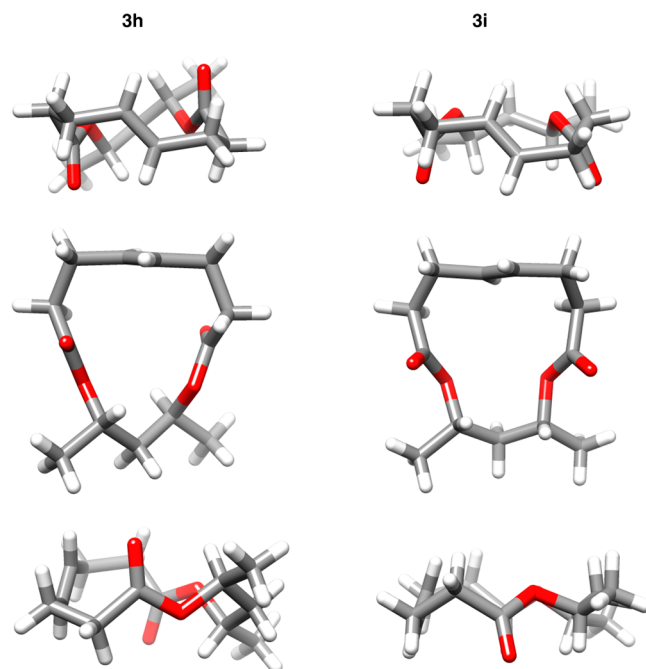


Figure 6. X-ray crystal structures of [13]-macrodialdehydes **3h** and **3i**.

CONCLUSION

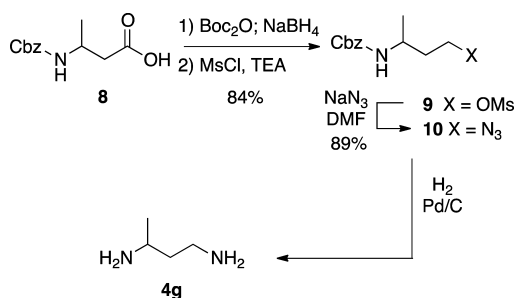
The structure and reactivity of the compounds investigated support some general trends that apply to this class of [13]-macrodialdehydes. Specifically, planar units such as esters, amides, and alkenes, among others, restrict the number of conformations populated in macrocyclic rings. The orientation or disposition of these planar units relative to one another is

mediated by bonds or atoms—referred to as hinges. The absolute stereochemistry at key centers along the macrocyclic backbone will influence how the planar units will organize themselves. Moreover, these key atoms work in tandem to drive the overall molecular topology. The observations made for this simple class of [13]-macrolidides also have implications for drug design as macrocycles have become the focus of several research efforts.¹ One area where the new chiral topology may be applied is the development of protein secondary structure mimetics. Additionally, the work described here provides a context for rationalizing the shape of natural product macrocycles.^{10,25} Our growing appreciation for the interplay among planar units, macrocyclic ring size, and the identification of key stereocenters has encouraged us to continue investigating these design principles in the contexts of other macrocyclic rings. Investigation of the biological activity of the [13]-macrolidides²⁶ and related structures is also ongoing.

EXPERIMENTAL SECTION

3-(*N*-Benzyloxycarbonyl)-amino-1-butyl Methanesulfonate (9). *N*-Cbz-3-amino butanoic acid **8** was converted to *N*-Cbz-3-aminobutanol according to a literature procedure (Scheme 3).²⁷ The alcohol (2.04 g, 9.2 mmol) and TEA (1.74 mL, 12.5 mmol) in dry DCM (50 mL) were cooled to 0 °C, to which MsCl (0.87 mL, 11.2 mmol) was added and stirred at the same temperature for 30 min. The whole reaction solution was then stirred overnight at room temperature. The solvent was removed under reduced pressure. The residue was purified by silica gel column chromatography (hexanes: EtOAc 60:40) to give **9** in 84% yield (2.33 g) as light yellow oil. *R*_f 0.43 (hexanes: EtOAc 6:4). ¹H NMR (400 MHz, CDCl₃): δ 7.32 (s, 5H), 5.05 (s, 2H), 5.01–4.90 (m, 1H), 4.22 (d, *J* = 4.0 Hz, 2H), 3.86 (d, *J* = 4.0 Hz, 1H), 2.92 (s, 3H), 1.85–1.82 (m, 2H), 1.18 (d, *J* = 4.0 Hz, 3H). ¹³C NMR (100 MHz, CDCl₃): δ 155.9, 136.6, 128.6, 128.2, 128.1, 67.4, 66.7, 44.2, 37.2, 36.3, 21.3. TOF HRMS (DART) *m/z* [M + H]⁺ calcd for C₁₃H₂₀NO₃S, 302.1062; found, 302.1063.

Scheme 3



3-(*N*-Benzyloxycarbonyl)-amino-1-butyl Azide (10). Under N₂, to a solution of **9** (1.18 g, 3.9 mmol) in dry DMF (10 mL) was added NaN₃ (1.27 g, 19.6 mmol), and the mixture was stirred at 70 °C overnight. H₂O (50 mL) and EtOAc (50 mL) were then added, and the EtOAc layer was washed with saturated NaHCO₃ (2 × 30 mL) and dried with Na₂SO₄. The solvent was removed under reduced pressure to give a residue which was purified by silica gel column chromatography (hexanes: EtOAc 85:15) to give **10** in 89% yield (0.87 g) as colorless oil. *R*_f 0.45 (hexanes: EtOAc 8:2). ¹H NMR (400 MHz, CDCl₃): δ 7.35 (s, 5H), 5.09 (s, 2H), 4.69 (d, *J* = 4.0 Hz, 1H), 3.86–3.83 (m, 1H), 3.37–3.34 (m, 2H), 1.73–1.70 (m, 2H), 1.20 (d, *J* = 8.0 Hz, 3H). ¹³C NMR (100 MHz, CDCl₃): δ 155.9, 136.6, 128.7, 128.4, 66.9, 48.6, 45.3, 36.2, 21.4. TOF HRMS (DART) *m/z* [M + H]⁺ calcd for C₁₂H₁₇N₄O₂, 249.1352; found, 249.1324.

1,3-Diamino Butane (4g). A mixture of **10** (0.86 g, 3.4 mmol), 10% Pd/C (85 mg), and methanol (10 mL) was stirred under a balloon of hydrogen at ambient pressure at rt overnight. The reaction

mixture was then filtered through a short plug of Celite and the filtrate was concentrated in vacuo to give crude **4g** (0.29 g) which was directly used in the preparation of **5g**. TOF HRMS (DART) *m/z* [M + H]⁺ calcd for C₄H₁₃N₂, 89.1078; found, 89.1080.

General Procedure for the Synthesis of Dienes. A solution of DCC (2.68 g, 0.013 mol) and DMAP (0.37 g, 0.0030 mmol) in dry DCM (40 mL) was cooled to 0 °C. To the solution, 4-pentenoic acid (1.24 mL, 12 mmol) was added, and the mixture was stirred at the same temperature for 30 min. The diol, amino alcohol, or diamine **1** (5 mmol) was then added to the mixture as a solution in dry DCM (10 mL). The suspension was stirred overnight at room temperature. The reaction mixture was then filtered and DCM was removed under reduced pressure. The residue was purified by silica gel column chromatography to give the diene products as described below.

Compound 5b. Obtained according to the general procedure in 90% yield (1.21 g) as colorless oil. *R*_f 0.51 (hexanes: EtOAc 8:2). ¹H NMR (400 MHz, CDCl₃): δ 5.74–5.68 (m, 2H), 5.45 (dd, *J* = 17.1, 1.2 Hz, 2H), 4.99 (dd, *J* = 10.4, 1.0 Hz, 2H), 3.79 (s, 1H), 2.31–2.28 (m, 8H), 0.87 (s, 6H). ¹³C NMR (100 MHz, CDCl₃): δ 172.6, 136.5, 115.4, 68.9, 34.6, 33.4, 28.8, 21.7. TOF HRMS (DART) *m/z* [M + H]⁺ calcd for C₁₅H₂₅O₄, 269.1753; found, 269.1716.

Compound 5c. Obtained according to the general procedure in 99% yield (1.32 g) as colorless oil. *R*_f 0.36 (EtOAc). ¹H NMR (400 MHz, CDCl₃): δ 6.64 (s, br, 2H), 5.86–5.76 (m, 2H), 5.35 (dd, *J* = 17.2, 1.2 Hz, 2H), 4.97 (dd, *J* = 10.0, 1.0 Hz, 2H), 2.97 (d, *J* = 8.0 Hz, 4H), 2.42–2.29 (m, 8H), 0.83 (s, 6H). ¹³C NMR (100 MHz, CDCl₃): δ 173.4, 137.1, 115.8, 45.8, 36.6, 36.2, 29.9, 23.8. TOF HRMS (DART) *m/z* [M + H]⁺ calcd for C₁₅H₂₆N₂O₂, 267.2073; found, 267.2071.

Compound 5d. Obtained according to the general procedure in 100% yield (1.43 g) as colorless oil. *R*_f 0.58 (hexanes: EtOAc 8:2). ¹H NMR (400 MHz, CDCl₃): δ 5.82–5.80 (m, 2H), 5.05 (m, 2H), 4.99 (m, 2H), 4.18 (t, *J* = 6.0 Hz, 1H), 2.38–2.32 (m, 8H), 2.13 (t, *J* = 8.0 Hz, 2H), 1.47 (s, 6H). ¹³C NMR (100 MHz, CDCl₃): δ 173.2, 172.4, 136.9, 136.8, 115.6, 80.9, 60.8, 39.4, 34.8, 33.7, 29.2, 28.9, 26.6. TOF HRMS (DART) *m/z* [M + NH₃]⁺ calcd for C₁₅H₂₅O₄NH₃, 286.2018; obs., 286.1973.

Compound 5e. Obtained according to the general procedure in 65% yield (0.82 g) as colorless oil. *R*_f 0.11 (hexanes: EtOAc 8:2). ¹H NMR (400 MHz, CDCl₃): δ 5.80–5.73 (m, 2H), 4.98 (m, 2H), 4.89 (m, 2H), 4.08–4.07 (m, 3H), 2.35–2.20 (m, 8H), 1.74–1.73 (m, 2H), 1.13 (d, *J* = 8.0 Hz, 3H). ¹³C NMR (100 MHz, CDCl₃): δ 173.2, 171.8, 137.2, 136.8, 115.7, 61.7, 42.8, 36.1, 35.6, 33.7, 29.9, 28.9, 21.1. TOF HRMS (DART) *m/z* [M + H]⁺ calcd for C₁₄H₂₄NO₃, 254.1756; found, 254.1744.

Compound 5f. Obtained according to the general procedure in 97% yield (1.23 g) as colorless oil. *R*_f 0.63 (hexanes: EtOAc 85:15). ¹H NMR (400 MHz, CDCl₃): δ 6.04 (s, br, 1H), 5.80–5.74 (m, 2H), 5.10 (dd, *J* = 17.3, 1.6 Hz, 2H), 4.95 (m, 3H), 3.46 (t, *J* = 8.0 Hz, 1H), 2.97–2.92 (m, 1H), 2.36–2.21 (m, 8H), 1.72–1.63 (m, 2H), 1.20 (d, *J* = 4.0 Hz, 3H). ¹³C NMR (100 MHz, CDCl₃): δ 173.1, 172.6, 137.2, 136.7, 115.8, 68.7, 36.0, 35.8, 33.9, 29.8, 29.1, 20.4. TOF HRMS (DART) *m/z* [M + H]⁺ calcd for C₁₄H₂₄NO₃, 254.1756; found, 254.1735.

Compound 5g. Obtained according to the general procedure in 46% yield (0.58 g) as pale yellow oil. *R*_f 0.1 (EtOAc). ¹H NMR (400 MHz, CDCl₃): δ 6.86 (s, br, 1H), 6.04 (d, *J* = 8.0 Hz, 1H), 5.80–5.70 (m, 2H), 5.02 (m, 1H), 4.98 (m, 1H), 4.93 (m, 2H), 3.99 (m, 1H), 3.59–3.58 (m, 1H), 2.73–2.67 (m, 1H), 2.34–2.22 (m, 8H), 1.65–1.63 (m, 1H), 1.32–1.26 (m, 1H), 1.19 (d, *J* = 4.0 Hz, 3H). ¹³C NMR (100 MHz, CDCl₃): δ 172.9, 172.5, 137.2, 136.9, 115.8, 115.4, 42.6, 37.2, 36.1, 35.9, 35.8, 29.8, 29.1, 21.3. TOF HRMS (DART) *m/z* [M + H]⁺ calcd for C₁₄H₂₅N₂O₂, 253.1916; found, 253.1928.

Compounds 5h/5i. The mixture of isomeric diesters was obtained according to the general procedure in 72% yield (0.96 g) as colorless oil. *R*_f 0.78 (hexanes: EtOAc 9:1). ¹H NMR (400 MHz, CDCl₃): δ 5.77–5.70 (m, 2H), 4.99–4.88 (m, 6H), 2.30 (d, *J* = 8.0 Hz, 8H), 1.94–1.53 (m, 2H), 1.15 (t, *J* = 4.0 Hz, 6H). ¹³C NMR (100 MHz, CDCl₃): δ 172.4, 136.7, 136.6, 115.5, 115.4, 67.8, 67.1, 42.4, 41.9, 33.8,

33.7, 28.9, 28.9, 20.5, 20.1. TOF HRMS (DART) m/z $[M + H]^+$ calcd for $C_{15}H_{25}O_4$, 269.1753; found, 269.1750.

General RCM Procedure. Under an atmosphere of dry N_2 , to a solution of diene **5** (1 mmol) in dry toluene (100 mL) was added Grubbs' second generation catalyst (0.05–0.08 mmol) and the resulting mixture was refluxed at 110 °C for 18 h. The toluene was removed under reduced pressure to give a residue, which was purified by silica gel column chromatography.

Compound 3b. Obtained according to the general procedure in 61% yield (0.146 g) as a white solid. mp 81–82 °C. R_f 0.65 (hexanes: EtOAc 8:2). 1H NMR (400 MHz, $CDCl_3$): δ 5.39 (d, J = 4.0 Hz, 2H), 3.79 (s, 4H), 2.31 (d, J = 8.0 Hz, 8H), 0.97 (s, 6H). ^{13}C NMR (100 MHz, $CDCl_3$): δ 173.9, 130.0, 69.2, 34.4, 33.5, 29.1, 22.9. TOF HRMS (DART) m/z $[M + H]^+$ calcd for $C_{13}H_{21}O_4$, 241.1440; found, 241.1444.

Compound 3c. Obtained according to the general procedure in 46% yield (0.110 g) as white solid. mp 91–93 °C. R_f 0.21 (EtOAc, 0.3% TEA). 1H NMR (400 MHz, $CDCl_3$): δ 6.12 (s, br, 2H), 5.56 (d, J = 4.0 Hz, 2H), 3.14 (d, J = 8.0 Hz, 4H), 2.31 (s, 8H), 0.93 (d, J = 8.0 Hz, 6H). ^{13}C NMR (100 MHz, $CDCl_3$): δ 173.3, 131.0, 49.3, 37.4, 35.5, 28.7, 24.8. TOF HRMS (DART) m/z $[M + H]^+$ calcd for $C_{13}H_{23}N_2O_2$, 239.1759; found, 239.1757.

Compound 3d. Obtained according to the general procedure in 67% yield (0.161 g) as white solid. mp 43–44 °C. R_f 0.63 (hexanes: EtOAc 8:2). 1H NMR (400 MHz, $CDCl_3$): δ 5.39–5.35 (m, 2H), 4.07 (t, J = 6.0 Hz, 2H), 2.29–2.16 (m, 10H), 1.36 (s, 6H). ^{13}C NMR (100 MHz, $CDCl_3$): δ 173.9, 172.2, 129.8, 129.5, 80.5, 60.5, 37.3, 34.9, 28.9, 27.6. TOF HRMS (DART) m/z $[M + H]^+$ calcd for $C_{13}H_{21}O_4$, 241.1440; found, 241.1410.

Compound 3e. Obtained according to the general procedure in 80% yield (0.181 g) as white solid. mp 85–87 °C. R_f 0.32 (EtOAc). 1H NMR (400 MHz, $CDCl_3$): δ 5.88 (s, br, 1H), 5.59–5.46 (m, 2H), 4.31 (t, J = 12.0 Hz, 1H), 4.20 (t, J = 12.0 Hz, 1H), 4.09–4.03 (m, 1H), 2.45–2.10 (m, 8H), 2.04–1.98 (m, 1H), 1.71–1.70 (m, 1H), 1.18 (d, J = 4.0 Hz, 3H). ^{13}C NMR (100 MHz, $CDCl_3$): δ 173.6, 171.9, 130.8, 130.6, 61.6, 43.7, 36.4, 34.7, 33.6, 28.1, 27.8, 20.7. TOF HRMS (DART) m/z $[M + H]^+$ calcd for $C_{12}H_{20}NO_3$; 226.1443; found, 226.1453.

Compound 3f. Obtained according to the general procedure in 61% yield (0.137 g) as white solid. mp 90–91 °C. R_f 0.30 (EtOAc). 1H NMR (400 MHz, $CDCl_3$): δ 6.02 (s, br, 1H), 5.53–5.49 (m, 2H), 5.03 (t, J = 12.0 Hz, 1H), 3.52–3.48 (m, 1H), 3.18–3.12 (m, 1H), 2.39–2.10 (m, 8H), 1.80–1.77 (m, 2H), 1.21 (d, J = 4.0 Hz, 3H). ^{13}C NMR (100 MHz, $CDCl_3$): δ 173.2, 172.9, 131.1, 130.9, 70.7, 37.1, 36.4, 34.9, 34.1, 28.2, 27.6, 20.9. TOF HRMS (DART) m/z $[M + H]^+$ calcd for $C_{12}H_{20}NO_3$, 226.1443; found, 226.1457.

Compound 3g. Obtained according to the general procedure in 72% yield (0.161 g) as white solid. mp 93–95 °C. R_f 0.05 (EtOAc, 0.5% TEA). 1H NMR (400 MHz, $CDCl_3$): δ 6.04 (s, br, 1H), 5.61 (s, br, 1H), 5.54 (d, J = 4.0 Hz, 2H), 4.12 (t, J = 4.0 Hz, 1H), 3.76 (t, J = 12.0 Hz, 1H), 3.04–2.97 (m, 1H), 2.38–2.15 (m, 8H), 1.78–1.76 (m, 1H), 1.66–1.64 (m, 1H), 1.19 (d, J = 8.0 Hz, 3H). ^{13}C NMR (100 MHz, $CDCl_3$): δ 172.9, 172.1, 130.9, 130.4, 44.9, 37.3, 37.0, 36.9, 35.8, 28.4, 28.2, 22.2. TOF HRMS (DART) m/z $[M + H]^+$ calcd for $C_{12}H_{21}N_2O_2$, 225.1603; found, 225.1597.

Compound 3h (racemate). Obtained according to the general procedure in 50% yield (0.120 g) as white solid. mp 116–117 °C. R_f 0.82 (hexanes: EtOAc 95:5). 1H NMR (400 MHz, $CDCl_3$): δ 5.41 (t, J = 4.0 Hz, 2H), 4.94–4.92 (m, 2H), 2.39–2.14 (m, 8H), 1.78 (t, J = 8.0 Hz, 2H), 1.24 (d, J = 4.0 Hz, 6H). ^{13}C NMR (100 MHz, $CDCl_3$): δ 173.1, 130.7, 67.2, 41.6, 34.6, 28.3, 20.5. TOF HRMS (DART) m/z $[M + H]^+$ calcd for $C_{13}H_{21}O_4$, 241.1440; found, 241.1444.

Compound 3i (meso). Obtained according to the general procedure in 26% yield (0.062 g) as white solid. mp 83–84 °C. R_f 0.78 (hexanes: EtOAc 9:1). 1H NMR (400 MHz, $CDCl_3$): δ 5.51 (s, 2H), 5.03–4.99 (m, 2H), 2.38–2.19 (m, 8H), 2.03–1.99 (m, 1H), 1.65 (d, J = 12.0 Hz, 1H), 1.20 (d, J = 4.0 Hz, 6H). ^{13}C NMR (100 MHz, $CDCl_3$): δ 173.1, 130.1, 70.6, 41.9, 35.3, 27.4, 21.9. TOF HRMS (DART) m/z $[M + H]^+$ calcd for $C_{13}H_{21}O_4$, 241.1440; found, 241.1446.

General Hydrogenation Procedure. A stirred mixture of macrocycle ring **4** (10 mg), 10% Pd/C (1 mg) in methanol (1 mL) was hydrogenated at ambient pressure (H_2 balloon) and rt for 3 h. The reaction mixture was then filtered through Celite, and the filtrate was concentrated in vacuo to give each product.

Compound 6a. Obtained according to the general procedure in 85% yield (9.0 mg) as a white solid. mp 37–38 °C. R_f 0.81 (hexanes: EtOAc 9:1). 1H NMR (400 MHz, $CDCl_3$): δ 5.08–5.04 (m, 1H), 4.29–4.24 (m, 1H), 4.09–4.04 (m, 1H), 2.31 (t, J = 6.0 Hz, 4H), 2.02–1.90 (m, 2H), 1.84–1.73 (m, 2H), 1.62–1.56 (m, 2H), 1.41–1.30 (m, 4H), 1.27 (d, J = 6.0 Hz, 3H). ^{13}C NMR (100 MHz, $CDCl_3$): δ 174.8, 174.0, 69.5, 61.8, 33.9, 33.8, 33.7, 26.6, 26.4, 24.8, 24.4, 20.9. TOF HRMS (DART) m/z $[M + H]^+$ calcd for $C_{12}H_{21}O_4$, 229.1440; found, 229.1429.

Compound 6b. Obtained according to the general procedure in 92% yield (9.0 mg) as a white solid. mp 73–74 °C. R_f 0.68 (hexanes: EtOAc 8:2). 1H NMR (400 MHz, $CDCl_3$): δ 3.82 (s, 4H), 2.36–2.24 (m, 4H), 1.66–1.63 (m, 4H), 1.27–1.24 (m, 4H), 0.96 (s, 6H). ^{13}C NMR (100 MHz, $CDCl_3$): δ 174.8, 70.4, 33.2, 28.9, 27.1, 23.1, 21.9. TOF HRMS (DART) m/z $[M + H]^+$ calcd for $C_{13}H_{23}O_4$, 243.1596; found, 243.1569.

Compound 6c. The compound was prepared according to the general procedure in 99% yield (10.0 mg) as a white solid. mp 161 °C (decomp). R_f 0.28 (EtOAc). 1H NMR (400 MHz, $CDCl_3$): δ 6.37 (s, br, 2H), 3.16 (d, J = 4.0 Hz, 4H), 2.28 (q, J = 4.0 Hz, 4H), 1.73 (t, J = 4.0 Hz, 4H), 1.41–1.38 (m, 4H), 0.94 (d, J = 12.0 Hz, 6H). ^{13}C NMR (100 MHz, $CDCl_3$): δ 173.9, 50.1, 36.8, 36.5, 27.4, 24.4, 21.9. TOF HRMS (DART) m/z $[M + H]^+$ calcd for $C_{13}H_{23}N_2O_2$, 241.1916; found, 241.1902.

Compound 6d. The compound was prepared according to the general procedure in 99% yield (10.0 mg) as a white solid. mp 79–80 °C. R_f 0.52 (hexanes: EtOAc 8:2). 1H NMR (400 MHz, $CDCl_3$): δ 4.17–4.13 (m, 2H), 2.28–2.07 (m, 6H), 1.61–1.54 (m, 4H), 1.51 (s, 6H), 1.47–1.43 (m, 4H), 0.88 (t, J = Hz, 3H). ^{13}C NMR (100 MHz, $CDCl_3$): δ 173.8, 173.1, 80.6, 60.6, 39.0, 35.7, 34.4, 28.9, 28.8, 26.7, 25.0, 24.9, 24.8. TOF HRMS (DART) m/z $[M + H]^+$ calcd for $C_{13}H_{23}O_4$, 243.1596; found, 243.1595.

Compound 6e. The compound was prepared according to the general procedure in 100% yield (10.0 mg) as a white solid. mp 107–108 °C. R_f 0.55 (hexanes: EtOAc 8:2). 1H NMR (400 MHz, $CDCl_3$): δ 5.52 (d, J = 4.0 Hz, 1H), 4.33 (td, J = 8.0, 4.0 Hz, 1H), 4.23–4.20 (m, 1H), 4.13 (td, J = 8.0, 4.0 Hz, 1H), 2.31–2.27 (m, 3H), 2.05–2.01 (m, 1H), 1.89–1.87 (m, 1H), 1.77–1.67 (m, 3H), 1.51–1.34 (m, 5H), 1.26 (d, J = 4 Hz, 3H). ^{13}C NMR (100 MHz, $CDCl_3$): δ 174.7, 172.4, 62.6, 44.7, 36.2, 34.4, 34.2, 27.4, 26.6, 24.5, 21.4. TOF HRMS (DART) m/z $[M + H]^+$ calcd for $C_{12}H_{22}NO_3$, 228.1600; found, 228.1596.

Compound 6f. The compound was prepared according to the general procedure in 98% yield (10.0 mg) as a white solid. mp 112–113 °C. R_f 0.58 (hexanes: EtOAc 7:3). 1H NMR (400 MHz, $CDCl_3$): δ 5.78 (s, br, 1H), 5.07–5.03 (m, 1H), 3.67–3.63 (m, 1H), 3.18–3.11 (m, 1H), 2.40–2.25 (m, 2H), 2.19 (t, J = 6.0 Hz, 2H), 1.90–1.70 (m, 6H), 1.46–1.39 (m, 4H), 1.26 (d, J = 8.0 Hz, 3H). ^{13}C NMR (100 MHz, $CDCl_3$): δ 174.3, 173.2, 71.5, 38.0, 36.2, 34.8, 34.0, 27.0, 26.2, 24.4, 23.7, 21.4. TOF HRMS (DART) m/z $[M + H]^+$ calcd for $C_{12}H_{22}NO_3$, 228.1600; found, 228.1588.

Compound 6g. The compound was prepared according to the general procedure in 98% yield (10.0 mg) as a white solid. mp 203–204 °C. R_f 0.18 (EtOAc). 1H NMR (400 MHz, $CDCl_3$): δ 6.33 (s, br, 1H), 5.75 (d, J = 8.0 Hz, 1H), 4.12–4.06 (m, 1H), 3.96–3.88 (m, 1H), 2.91–2.88 (m, 1H), 2.37–2.21 (m, 3H), 2.08 (td, J = 8.0, 4.0 Hz, 1H), 1.91–1.81 (m, 1H), 1.71–1.36 (m, 9H), 1.18 (d, J = 8.0 Hz, 3H). ^{13}C NMR (100 MHz, $CDCl_3$): δ 173.4, 172.6, 45.3, 37.5, 36.9, 36.2, 36.0, 26.9, 26.2, 23.2, 22.5, 22.3. TOF HRMS (DART) m/z $[M + H]^+$ calcd for $C_{12}H_{23}N_2O_2$, 227.1760; found, 227.1768.

Compound 6h (racemate). Obtained according to the general procedure in 88% yield (9.0 mg) as a white solid. mp 123–124 °C. R_f 0.79 (hexanes: EtOAc 9:1). 1H NMR (400 MHz, $CDCl_3$): δ 5.11 (dd, J = 16.0, 8.0 Hz, 2H), 2.31 (q, J = 4.0 Hz, 4H), 1.92 (t, J = 4.5 Hz, 2H), 1.85–1.81 (m, 2H), 1.56–1.50 (m, 3H), 1.42–1.36 (m, 3H), 1.28 (d, J

= 4.0 Hz, 6H). ^{13}C NMR (100 MHz, CDCl_3): δ 174.1, 67.6, 40.9, 33.4, 25.9, 24.4, 20.8. TOF HRMS (DART) m/z $[\text{M} + \text{H}]^+$ calcd for $\text{C}_{13}\text{H}_{23}\text{O}_4$, 243.1596; found, 243.1572.

Compound 6i (meso). Obtained according to the general procedure in 99% yield (10.0 mg) as a white solid. mp 117–118 °C. R_f 0.73 (hexanes: EtOAc 9:1). ^1H NMR (400 MHz, CDCl_3): δ 5.02–4.98 (m, 2H), 2.31 (t, $J = 8.0$ Hz, 4H), 2.13–2.09 (m, 1H), 1.70–1.61 (m, 5H), 1.36 (d, $J = 4.0$ Hz, 4H), 1.23 (d, $J = 4.0$ Hz, 6H). ^{13}C NMR (100 MHz, CDCl_3): δ 174.4, 71.1, 42.1, 34.9, 27.6, 24.1, 21.8. TOF HRMS (DART) m/z $[\text{M} + \text{H}]^+$ calcd for $\text{C}_{13}\text{H}_{23}\text{O}_4$, 243.1596; found, 243.1607.

General Epoxidation Procedure. Following the literature procedure,⁷ to a solution of **3** (10 mg) in acetone– H_2O :DCM (1:1:1, 9 mL) was added excess amount of NaHCO_3 (100 mg, 0.94 mmol) and Oxone (120 mg, 0.19 mmol) at 0 °C. The resulting heterogeneous solution was stirred for 3 h at 0 °C, and extracted with DCM. After removal of the solvent, the residue was purified by chromatography to give the epoxide product.

Compound 7a. Obtained according to the general procedure in 93% yield (10.0 mg) as a white solid. mp 91–92 °C. R_f 0.56 (hexanes: EtOAc 7:3). ^1H NMR (400 MHz, CDCl_3): δ 5.28–5.22 (m, 1H), δ 4.72 (td, $J = 8.0, 4.0$ Hz, 1H), 3.83–3.79 (m, 1H), 2.78 (d, $J = 8.0$ Hz, 1H), 2.71 (d, $J = 8.0$ Hz, 1H), 2.42–2.39 (m, 4H), 2.23–2.07 (m, 3H), 1.82–1.75 (m, 1H), 1.58–1.48 (m, 2H), 1.26 (d, $J = 4.0$ Hz, 3H). ^{13}C NMR (100 MHz, CDCl_3): δ 172.8, 69.0, 58.2, 34.6, 29.6, 26.9, 22.9. TOF HRMS (DART) m/z $[\text{M} + \text{H}]^+$ calcd for $\text{C}_{12}\text{H}_{18}\text{O}_5$, 243.1233; found, 243.1221.

Compound 7b. The compound was prepared according to the general procedure in 88% yield (9.0 mg) as a white solid. mp 105–106 °C. R_f 0.62 (hexanes: EtOAc 8:2). ^1H NMR (400 MHz, CDCl_3): δ 4.49 (d, $J = 8.0$ Hz, 2H), 3.38 (d, $J = 12.0$ Hz, 2H), 2.72 (d, $J = 8.0$ Hz, 2H), 2.41–2.36 (m, 4H), 2.19–2.14 (m, 2H), 1.60–1.54 (m, 2H), 1.02 (s, 6H). ^{13}C NMR (100 MHz, CDCl_3): δ 172.8, 69.0, 58.2, 34.6, 29.6, 26.9, 22.9. TOF HRMS (DART) m/z $[\text{M} + \text{H}]^+$ calcd for $\text{C}_{13}\text{H}_{21}\text{O}_5$, 257.1389; found, 257.1360.

Compound 7c. The compound was prepared according to the general procedure in 81% yield (9.0 mg) as a white solid. mp 157–158 °C. R_f 0.20 (hexanes: EtOAc 6:4). ^1H NMR (400 MHz, CDCl_3): δ 6.28 (s, br, 2H), 3.43 (dd, $J = 12.0, 8.0$ Hz, 2H), 2.88 (dd, $J = 12.0, 8.0$ Hz, 2H), 2.76 (d, $J = 8.0$ Hz, 2H), 2.41 (t, $J = 6.0$ Hz, 2H), 2.38–2.34 (m, 2H), 2.23–2.16 (m, 2H), 1.90–1.66 (m, 2H), 1.47–1.43 (m, 2H), 0.94 (s, 6H). ^{13}C NMR (100 MHz, CDCl_3): δ 172.9, 57.9, 48.8, 36.1, 32.8, 27.6, 25.0. TOF HRMS (DART) m/z $[\text{M} + \text{H}]^+$ calcd for $\text{C}_{13}\text{H}_{23}\text{N}_2\text{O}_3$, 255.1709; found, 255.1738.

Compound 7d. The compound was prepared according to the general procedure in 77% yield (8.0 mg) as a white solid. mp 83–84 °C. R_f 0.58 (hexanes: EtOAc 8:2). ^1H NMR (400 MHz, CDCl_3): δ 4.36 (q, $J = 4.0$ Hz, 1H), 4.28 (q, $J = 4.0$ Hz, 1H), 2.86 (d, $J = 8.0$ Hz, 1H), 2.77 (d, $J = 8.0$ Hz, 1H), 2.39–2.23 (m, 8H), 1.59–1.50 (m, 2H), 1.45 (d, $J = 8.0$ Hz, 6H). ^{13}C NMR (100 MHz, CDCl_3): δ 173.0, 172.3, 81.1, 60.7, 57.7, 57.4, 37.9, 31.5, 31.2, 27.5, 27.3, 27.0, 26.3. TOF HRMS (DART) m/z $[\text{M} + \text{H}]^+$ calcd for $\text{C}_{13}\text{H}_{21}\text{O}_5$, 257.1389; found, 257.1360.

Compound 7e. The compound was prepared according to the general procedure in 93% yield (10.0 mg) as a white solid. mp 101–102 °C. R_f 0.55 (hexanes: EtOAc 6:4). ^1H NMR (400 MHz, CDCl_3): δ 5.58 (d, $J = 4.0$ Hz, 0.25H), 5.22 (d, $J = 8.0$ Hz, 0.75H), 4.69 (td, $J = 12.0, 4.0$ Hz, 1H), 4.66–4.10 (m, 1H), 3.89 (td, $J = 8.0, 4.0$ Hz, 1H), 2.84–2.81 (m, 1H), 2.67–2.64 (m, 1H), 2.45–2.41 (m, 1H), 2.39–2.06 (m, 5H), 1.75–1.40 (m, 4H), 1.20 (d, $J = 4.0$ Hz, 0.8H), 1.16 (d, $J = 4.0$ Hz, 2.2H). ^{13}C NMR (100 MHz, CDCl_3): δ 170.6, 60.1, 58.9, 58.4, 41.9, 34.1, 31.5, 29.8, 27.0, 26.7, 22.0. TOF HRMS (DART) m/z $[\text{M} + \text{H}]^+$ calcd for $\text{C}_{12}\text{H}_{20}\text{NO}_4$, 242.1392; found, 242.1416.

Compound 7f. The compound was prepared according to the general procedure in 76% yield (8.0 mg) as a white solid. mp 115–116 °C. R_f 0.11 (DCM: EtOAc: methanol 80:15:5). ^1H NMR (400 MHz, CDCl_3): δ 5.35 (d, $J = 4.0$ Hz, 1H), 5.24 (td, $J = 8.0, 4.0$ Hz, 1H), 3.91–3.85 (m, 1H), 3.04 (dd, $J = 12.0, 8.0$ Hz, 1H), 2.78 (t, $J = 8.0$ Hz, 2H), 2.44 (q, $J = 4.0$ Hz, 2H), 2.32–2.30 (m, 1H), 2.20–2.11 (m, 3H), 1.86–1.80 (m, 2H), 1.69–1.59 (m, 2H), 1.22 (d, $J = 4.0$ Hz,

3H). ^{13}C NMR (100 MHz, CDCl_3): δ 172.8, 171.3, 66.8, 59.2, 58.5, 35.2, 33.6, 31.8, 29.6, 27.2, 26.5, 20.8. TOF HRMS (DART) m/z $[\text{M} + \text{H}]^+$ calcd for $\text{C}_{12}\text{H}_{20}\text{NO}_4$, 242.1392; found, 242.1417.

Compound 7h (racemate). The compound was prepared according to the general procedure in 94% yield (10.0 mg) as a white solid. mp 97–98 °C. R_f 0.70 (hexanes: EtOAc 7:3). ^1H NMR (400 MHz, CDCl_3): δ 5.23–5.18 (m, 2H), 2.73 (d, $J = 8.0$ Hz, 2H), 2.43–2.35 (m, 4H), 2.15 (td, $J = 12.0, 4.0$ Hz, 2H), 1.82 (t, $J = 8.0$ Hz, 2H), 1.54–1.51 (m, 2H), 1.22 (d, $J = 8.0$ Hz, 6H). ^{13}C NMR (100 MHz, CDCl_3): δ 172.4, 161.4, 66.8, 59.0, 29.6, 26.8, 20.4. HRMS m/z $[\text{M} + \text{H}]^+$ calcd for $\text{C}_{13}\text{H}_{21}\text{O}_5$, 257.1389; found, 257.1365.

Compound 7i (meso). The compound was prepared according to the general procedure in 91% yield (10.0 mg) as a white solid. mp 109–110 °C. R_f 0.75 (hexanes: EtOAc 7:3). ^1H NMR (400 MHz, CDCl_3): δ 5.22–5.18 (m, 2H), 2.96 (q, $J = 4.0$ Hz, 1H), 2.72 (q, $J = 4.0$ Hz, 1H), 2.50–2.17 (m, 6H), 2.02–1.96 (m, 1H), 1.65–1.53 (m, 3H), 1.24 (d, $J = 8.0$ Hz, 6H). ^{13}C NMR (100 MHz, CDCl_3): δ 176.6, 71.0, 70.8, 57.0, 56.6, 42.4, 32.0, 30.7, 27.1, 26.4, 21.9, 21.8. TOF HRMS (DART) m/z $[\text{M} + \text{H}]^+$ calcd for $\text{C}_{13}\text{H}_{21}\text{O}_5$, 257.1389; found, 257.1367.

■ ASSOCIATED CONTENT

● Supporting Information

Crystallographic data for **3h**, **3i**, **7b**, and **7d** are in the Cambridge Crystallographic Data Centre (CCDC), 924286, 924287, 924284, and 924285. Copies of this information may be obtained free of charge from CCDC, 12 Union Road, Cambridge CB2 1EZ, UK (Fax: +44–1223–336033; web: www.ccdc.cam.ac.uk/conts/retrieving/html; e-mail: deposit@ccdc.cam.ac.uk). VT ^1H NMR data for **3h** and **6h** and characterization data including ^1H and ^{13}C NMR spectra of all new compounds. This material is available free of charge via the Internet at <http://pubs.acs.org>.

■ AUTHOR INFORMATION

Corresponding Author

*E-mail: mark.peczuh@uconn.edu.

Notes

The authors declare no competing financial interest.

■ ACKNOWLEDGMENTS

We thank Daniel Terwilliger for initial experiments on this project. The NSF supported this work through a grant to M.W.P. (CHE-0957626). 400 MHz/100 MHz NMR spectra were collected on an instrument that was upgraded by an NSF-CRIF grant (CHE-0947019). Michael Takase at the Chemistry Instrumentation Center at Yale University is acknowledged for collection of X-ray data on **3h**, **3i**, **7b**, and **7d**. Carlos Pacheco is acknowledged for assistance collecting NMR spectra, especially the VT ^1H NMR data on **3h** and **6h**.

■ REFERENCES

- (1) (a) Mallison, J.; Collins, I. *Future Med. Chem.* **2012**, *4*, 1409–1438. (b) Madsen, C. M.; Clause, M. H. *Eur. J. Org. Chem.* **2011**, 3107–3115. (c) Brandt, W.; Haupt, V. J.; Wessjohann, L. A. *Curr. Top. Med. Chem.* **2010**, *10*, 1361–1379. (d) Kotz, J. *SciBX* **2012**, *5*, doi:10.1038/scibx.2012.1176 (February 2013).
- (2) Driggers, E. M.; Hale, S. P.; Lee, J.; Terrett, N. K. *Nat. Rev. Drug Disc.* **2008**, *7*, 608–624.
- (3) Retsema, J.; Girard, A.; Schelkly, W.; Manousos, M.; Anderson, M.; Bright, G.; Borovoy, R.; Brennan, L.; Mason, R. *Antimicrob. Agents Chemother.* **1987**, *31*, 1939–1947.
- (4) (a) Walensky, L. D.; Kung, A. L.; Escher, I.; Malia, T. J.; Barbutto, S.; Wright, R. D.; Wagner, G.; Verdine, G. L.; Korsmeyer, S. J. *Science* **2004**, *305*, 1466–1470. (b) Schafmeister, C. E.; Po, J.; Verdine, G. L. J.

- Am. Chem. Soc.* **2000**, *122*, 5891–5892. (c) Judice, J. K.; Tom, J. Y. K.; Huang, W.; Wrin, T.; Vennari, J.; Petropoulos, C. J.; McDowell, R. S. *Proc. Natl. Acad. Sci., U. S. A.* **1997**, *94*, 13426–13430.
- (5) (a) Kopp, F.; Stratton, C. F.; Akella, L. B.; Tan, D. S. *Nat. Chem. Biol.* **2012**, *8*, 358–365. (b) Wessjohann, L. A.; Rivera, D. G.; Vercillo, O. E. *Chem. Rev.* **2009**, *109*, 796–814. (c) Schmidt, D. R.; Kwon, O.; Schreiber, S. L. *J. Comb. Chem.* **2004**, *6*, 286–292.
- (6) (a) Stanton, B. A.; Peng, L. F.; Maloof, N.; Nakai, K.; Wang, X.; Duffner, J. L.; Taveras, K. M.; Hyman, J. M.; Lee, S. W.; Koehler, A. N.; Chen, J. K.; Fox, J. L.; Mandinova, A.; Schreiber, S. L. *Nat. Chem. Biol.* **2009**, *5*, 154–156. (b) Metaferia, B. B.; Chen, L.; Baker, H. L.; Huang, X. Y.; Bewley, C. A. *J. Am. Chem. Soc.* **2007**, *129*, 2434–2435.
- (7) Lee, D.; Sello, J. K.; Schreiber, S. L. *J. Am. Chem. Soc.* **1999**, *121*, 10648–10649.
- (8) Schreiber, S. L. *Science* **2000**, *287*, 1964–1968.
- (9) (a) Sello, J. K.; Andreana, P. R.; Lee, D.; Schreiber, S. L. *Org. Lett.* **2003**, *5*, 4125–4127. (b) Blankenstein, J.; Zhu, J. *Eur. J. Org. Chem.* **2005**, 1949–1964.
- (10) (a) Caleta, I.; Cikos, A.; Zihner, D.; Dilovic, I.; Duksi, M.; Gembarovski, D.; Grgicevic, I.; Krajacic, M. B.; Filic, D.; Matkovic-Calogovic, D.; Malnar, I.; Alihodizic, S. *Struct. Chem.* **2012**, *23*, 1785–1796. (b) Kang, E. J.; Lee, E. *Chem. Rev.* **2005**, *105*, 4348–4378.
- (11) Fyvie, W. S.; Pecuh, M. W. *Chem. Commun.* **2008**, 4028–4030.
- (12) Fyvie, W. S.; Pecuh, M. W. *J. Org. Chem.* **2008**, *73*, 3626–3629.
- (13) (a) Han, C.; Rangarajan, S.; Voukides, A.; Beeler, A. B.; Johnson, R.; Porco, J. A. *Org. Lett.* **2009**, *11*, 413–416. (b) Still, W. C.; Romero, A. G. *J. Am. Chem. Soc.* **1986**, *108*, 2105–2106. (c) Arns, S.; Lebrun, M.; Grise, C. M.; Denissova, I.; Barriault, L. *J. Org. Chem.* **2007**, *72*, 9314–9322. (d) Still, W. C.; Galynker, I. *Tetrahedron* **1981**, *37*, 3981–3996.
- (14) Eliel, E. L.; Wilen, S. H. Chirality in Molecules Devoid of Chiral Centers. In *Stereochemistry of Organic Compounds*; John Wiley & Sons: New York, 1994; pp 1172–1175.
- (15) The synthesis of **3a** was previously reported. See ref 11.
- (16) (a) Lai, M. H. Y.; Brimble, M. A.; Callis, D. J.; Harris, P. W. R.; Levi, M. S.; Sieg, F. *Bioorg. Med. Chem.* **2005**, *13*, 533–548. (b) Tully, D. C.; Liu, H.; Alper, P. B.; Chatterjee, A. K.; Epple, R.; Roberts, M. J.; Williams, J. A.; Nguyen, K. L. T.; Woodmansee, D. H.; Tumanut, C.; Li, J.; Spraggon, G.; Chang, J.; Tuntland, T.; Harris, J. L.; Karanewsky, D. S. *Bioorg. Med. Chem. Lett.* **2006**, *16*, 1975–1980.
- (17) Bogdan, A. R.; Jerome, S. V.; Houk, K. N.; James, K. J. *Am. Chem. Soc.* **2012**, *134*, 2127–138.
- (18) Variable temperature ^1H NMR spectra of **3h** and **6h** are in the Supporting Information.
- (19) (a) Nubbemeyer, U. *Eur. J. Org. Chem.* **2001**, 1801–1816. (b) Dieters, A.; Mück-Lichtenfeld, C.; Fröhlich, R.; Hoppe, D. *Chem.—Eur. J.* **2002**, *8*, 1833–1842. (c) Sudau, A.; Münch, W.; Bats, J. W.; Nubbemeyer, U. *Chem.—Eur. J.* **2001**, *7*, 611–621. (d) Sudau, A.; Münch, W.; Nubbemeyer, U. *J. Org. Chem.* **2000**, *65*, 1710–1720.
- (20) 2,4-Pentanediol is commercially available as ~3:2 mixture of the (racemic:meso) diastereomers.
- (21) Ikeda, H.; Sato, E.; Sugai, T.; Ohta, H. *Tetrahedron* **1996**, *52*, 8113–8122.
- (22) Standard *m*CPBA epoxidation was also attempted on **3g**; the disappearance of starting material (TLC) without the appearance of a clear product in either epoxidation reaction suggested decomposition. Reactions of [13]-macrolactones (e.g., **3a**, **3b**, and **3d**) were slightly lower than the in situ DMDO method. Reactions with *m*CPBA and nitrogen containing [13]-macrolactones were unsuccessful.
- (23) Fyvie, W. S. Synthesis and Reactivity of Olefinic Carbohydrate-Derived Natural Product Analogs. Ph.D. Thesis, University of Connecticut, Storrs, CT 2009.
- (24) Supporting Information Figure S2a illustrates the difference in orientations of the C8–C11 unit.
- (25) Molinski, T. F.; Morinaka, B. I. *Tetrahedron* **2012**, *68*, 9307–9343.
- (26) Magpusao, A.; Desmond, R. T.; Billings, K. J.; Fenteany, G.; Pecuh, M. W. *Bioorg. Med. Chem. Lett.* **2010**, *20*, 5472–5476.
- (27) Davies, S. B.; McKervey, M. A. *Tetrahedron Lett.* **1999**, *40*, 1229–1232.